Simulating the Embolization of Blood Vessels Using Magnetic Microparticles and Acupuncture Needle in a Magnetic Field

Ovidiu Rotariu,*,† Gheorghe Iacob,‡ Norval J. C. Strachan,† and Horia Chiriac§

School of Biological Sciences, University of Aberdeen, Aberdeen AB24 3UU, Scotland, U.K., University of Medicine and Pharmacy, Faculty of Medical Bioengineering, Strada Universitatii, no. 16, Iasi 700115, Romania, and National Institute of R-D for Technical Physics, Bd. Mangeron no. 47, Iasi 700050, Romania

Computer models were developed to simulate the capture and subsequent deposition of magnetic microparticles (MMPs) in a blood vessel adjacent to a ferromagnetic wire (e.g., acupuncture needle) magnetized by a uniform external magnetic field. Process parameter conditions were obtained to enable optimal capture of MMPs into the deposit. It was found that the maximum capture distance of the MMPs was within 0.5−2.0 mm when the particles were superparamagnetic and had large size (>1.0 μm) and relative large flow rates (2.5−5.0 cm/s) as in a healthy artery. It was also found that the deposits were asymmetrical and that their size was between 1.0 and 2.0 mm. For the case of lower flow rates as can be found in a tumor (<1.0 mm/s) and using small magnetite particles (0.25−2.0 μm) the maximum capture distance was larger, ranging between approximately 0.5 and 6.4 mm, depending on the blood flow rate, the radius of wire, and particle clustering. The range of embolization (deposition) in this later case was between 0.5 and 5.9 mm. The potential of this technique to generate MMPs deposits to embolize blood vessels inhibiting the blood supply and thus facilitating necrosis of tumors located deep within the patient (3−7 cm) is discussed.

Introduction

Magnetic particles of colloidal and micrometer size have become of increasing importance in the past 15 years, with applications in industrial processing, biotechnology, microbiology, and medicine (*1*−*10*). Medical applications for magnetic particles include tumor targeting (associated with chemotherapeutic drugs, radiopharmaceutical agents, and magnetic fluid hyperthermia), immunomagnetic tests, and magnetic resonance imaging (*11*−*15*).

A technique used in tumor therapy involves embolization of blood vessels to inhibit the blood supply to the tumor to facilitate its necrosis. In its simplest form this comprises the injection of poly(vinyl alcohol) particles into the blood vessel through a catheter (*16*). Recently in vitro techniques of blood embolization in cancer treatment have been developed with magnetorheological fluids (*17*, *18*). However, it is difficult to obtain selective embolization of small blood vessels when these are positioned at a large distance from the magnetic field source (e.g., approximately >3 cm inside the body of the patient). What is required is a suitable magnetic field intensity and gradient in the vicinity of the vessel that enables concentration of the magnetic field lines and hence magnetic particles where the embolization is required.

A possible solution to this problem may be obtained by inserting ferromagnetic wires, for example, acupuncture needles (Seirin Co., Ltd.), close to the blood vessel. These ferromagnetic wires, with diameter approximately 0.5 mm and length up to 70 mm, will induce a large magnetic field gradient when a uniform external magnetic field is applied (*19*). This magnetic field gradient will induce strong magnetic forces on MMPs inoculated into the patients' blood, causing the MMPs to deposit on the vessels wall close to the ferromagnetic wire and thus enabling embolization to take place.

Magnetic carriers can be used as a drug delivery system when they are coupled with chemotherapeutic drugs (*11*) or labeled with radiopharmaceutical agents (*20*). However, this can be difficult to achieve effectively for tumors that are difficult to access (*12*) and where the delivery of drugs could improve the efficiency of therapy. Preliminary studies on high gradient magnetic capture of ferrofluids and its implications for drug targeting and tumor embolization have been made (*21*). Using these methods it is possible to capture superparamagnetic nanoparticles, but the capture of small particles (<40 nm) is affected by thermal fluctuations and the parameters of the capturing process must be carefully chosen to avoid this drawback.

In this study, we present a model that simulates the motion and deposition of MMPs in a blood vessel in the presence of a high magnetic field gradient generated around a magnetized ferromagnetic wire. We optimize the system parameters (MMP size, magnetic susceptibility, clustering formation, size of the ferromagnetic wire, and intensity of the external magnetic field) taking into account conditions specific for blood flow (i.e., viscosity and velocity).

* To whom correspondence should be addressed. Tel: +44(0)-1224 272256. Fax: +44(0)1224 272703. Email: o.rotariu@abdn.ac.uk.

† University of Aberdeen.

‡ University of Medicine and Pharmacy.

§ National Institute of R-D for Technical Physics.

10.1021/bp034146o CCC: $27.50
Published on Web 09/17/2003

Modeling and Simulation

Specifications. The following specifications are made in generating the models:

- the superparamagnetic or ferromagnetic MMPs have spherical shape and are magnetized in the magnetic field around the ferromagnetic wire;
- the MMPs are suspended in the carrier fluid (blood) at volume fractions less than 0.1% (larger volume fractions have been found to contain large clumps of particles that settle under gravity before they reach the target artery to be embolized (*17*, *18*));
- as a result of dipolar magnetic interactions the MMPs can build clusters; the maximum dimensions of the clusters considered here is five particles/cluster (*22*);
- the carrier fluid flow is laminar and as such only the average velocity is considered in the simulations;
- the ferromagnetic wire has cylindrical shape, is magnetized at saturation, and is positioned outside the blood vessel, mutually perpendicular to the blood flow and the background magnetic field, respectively;
- the interaction forces between MMPs that are simulated are (i) magnetic interaction between particles or clusters and the magnetized wire, (ii) hydrodynamic interaction between particles or clusters and the carrier fluid, and (iii) contact point interaction between MMPs in blood and MMPs on the surface of the deposit in the blood vessel;
- both inertial and gravity forces are neglected because the particles are micrometer size;

Models. ***(a) Motion and Deposition of MMPs in a Blood Vessel.*** The motion of MMPs in a blood vessel and their subsequent deposit onto the wall adjacent to the ferromagnetic wire is obtained by the method of trajectories (*23*). Figure 1. shows how MMPs carried by the blood are deviated toward the region with highest magnetic field intensity and are thus deposited onto the vessel's wall.

The equation for the MMPs motion when subjected to the action of both magnetic and hydrodynamic drag forces is (*24*)

$$\frac{dy_a}{dt} = \frac{v_{mp}}{a} f_1(K, y_a, z_a) \tag{1a}$$

$$\frac{dz_a}{dt} = -\frac{v_0}{a} + \frac{v_{mp}}{a} f_2(K, y_a, z_a) \tag{1b}$$

In eq 1 (a, b) the position at every moment t for a MMP (or cluster) is given by (y_a, z_a) coordinates that are normalized to the radius of the ferromagnetic wire, a. The functions f_1 and f_2 have a nonlinear dependence with the position of MMP (cluster) and are also dependent on the magnetic properties of the ferromagnetic wire by the magnetization factor

$$K = \frac{M_s}{2H_0} \tag{2}$$

where M_s is the magnetization of ferromagnetic wire at its magnetic saturation, and H_0 is the intensity of background magnetic field. The magnetic velocity of the MMP (cluster) is denoted by v_{mp} and mean velocity of blood in the artery by v_0. The magnetic velocity of the MMP (cluster) is the terminal velocity that the MMP (cluster) attains under the influence of both magnetic and hydrodynamic drag forces. This is given by (*23*)

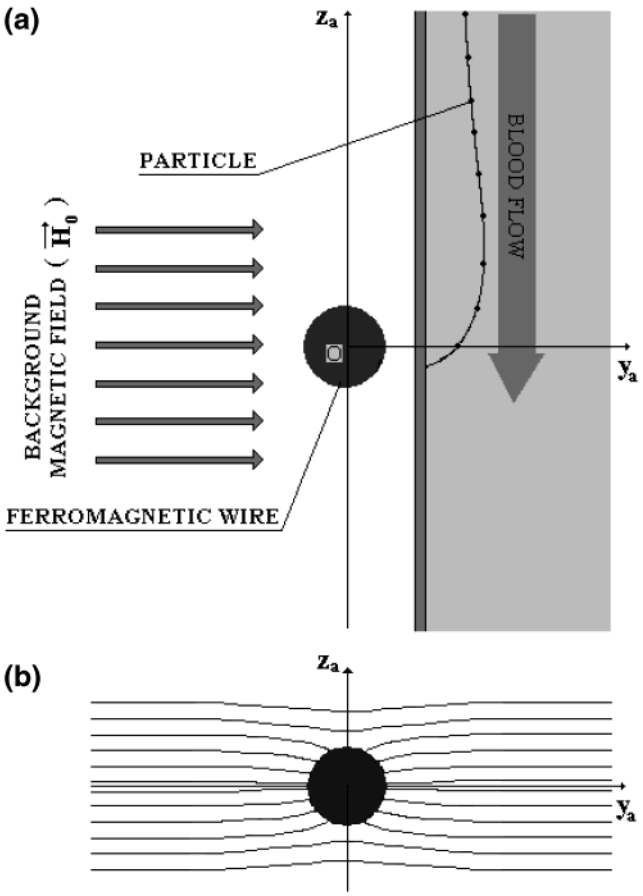

Figure 1. (a) Schematic illustrating the trajectory and deposition of an MMP in a blood vessel and (b) magnetic field lines around the ferromagnetic wire.

$$v_{mp} = \frac{4}{9} \frac{\mu_0 \chi b^2 K H_0^2}{\eta_f a} \tag{3}$$

where μ_0 is the magnetic permeability of void space, χ is the magnetic susceptibility of a particle, b is its radius, a is the radius of ferromagnetic wire, and η_f is the blood viscosity.

The system of differential equations given by eqs 1 is nonlinear and their numerical solution yields the trajectories of the MMPs (clusters).

(b) Stability and Limits of MMPs Deposit in a Blood Vessel. The stability and limit of the MMPs deposit in blood vessels under the presence of a magnetized ferromagnetic wire was simulated by modeling at equilibrium the forces acting on the MMPs (*25*).

For the case of the transverse configuration illustrated in Figure 2, the radial limit of the deposit may imply the presence of an extra static frictional force between particles and deposit. This force acts against the tangential component of the hydrodynamic drag force that tends to push the particles out of the deposit. No analytic expression for this static frictional coefficient has been developed, but for some particular cases experimental values have been calculated (*26*).

To avoid incorporation of this static frictional force we calculate the limits of the deposit at the equilibrium conditions when the radial forces acting on the MMPs and the moment of the total force ($\vec{F}$) related to a contact point between particle and deposit are ≤ 0 (Figure 2). Neglecting the effects of gravity and interaction between particles, a MMP located on the outermost layer on the surface of the deposit is subject to the action of the

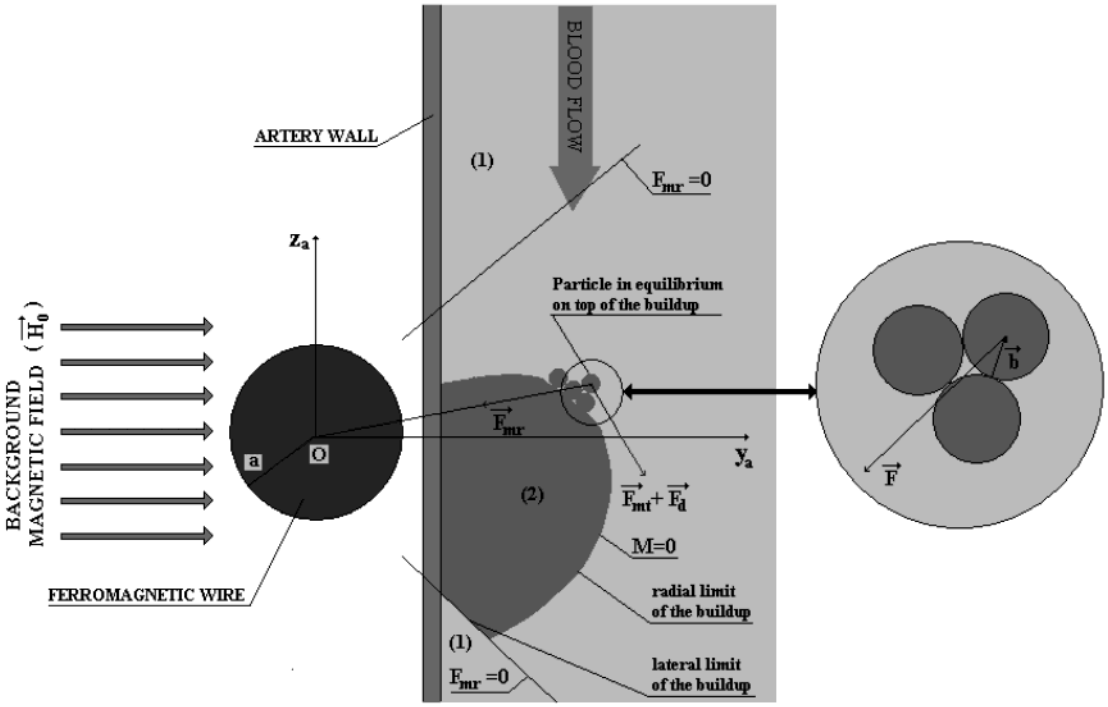

Figure 2. Equilibrium for particles located on top of the deposit. A particle having positive magnetic susceptibility is at equilibrium if the radial force and the moment of the total force acting on a contact point are ≤0.

nonuniform magnetic field (F_{mr} and F_{mt}, the radial and tangential components of the magnetic force) and to the hydrodynamic drag force (F_d).

The first requirement for a positive magnetic susceptible particle to remain on the buildup is

$$F_{mr} \leq 0 \tag{4}$$

The condition $F_{mr} = 0$ splits the space around the ferromagnetic magnetized wire into two capturing regions, one for negative magnetic susceptible particles (marked with 1) and another for positive magnetic susceptible particles (marked with 2) (Figure 2). The relation (eq 4) states the condition for the lateral limit of the buildup of MMPs.

The second requirement for the equilibrium of MMP, proposed here, is that the moment of the total force acting on the particle, at the point of contact between the particle and deposit, be ≤0, i.e.

$$\vec{M} = \vec{F} \times \vec{b} \leq 0 \tag{5}$$

A positive value for M could enable motion of the particle on the deposit until it finds a stable place ($M \leq 0$) or, alternately, its escape from the influence of the magnetic force and its removal from the deposit. The condition $M = 0$ gives the radial limit of the deposit of MMPs.

Parameters. Model simulations were performed for different values of the process parameters: (i) the radius of ferromagnetic wire ($a = 0.15 \times 10^{-3}$, 0.25×10^{-3}, and 0.5×10^{-3} m); (ii) $K = 0.9$; (iii) the radius of MMPs ($b = 0.125 \times 10^{-6}$ to 2.25×10^{-6} m); (iv) the magnetic susceptibility of MMPs ($\chi = 0.25$, 1.6, and 80.0); (v) the magnetization of magnetite particles ($M_p = 416\,000$ A/m); (vi) the intensity of the background uniform magnetic field ($H_0 = 40 \times 10^4$, 64×10^4, and 80×10^4 A/m); (vii) the dynamic viscosity of blood for a 40% hematocrit ($\eta_f = 0.028$ kg/ms); (viii) the mean velocity of blood flow ($v_0 = 10^{-4}$ to 5×10^{-2} m/s).

Simulations. Equations 1 were solved numerically using a fourth-order Runge−Kutta method (*27*). The trajectories of particles were determined for flow conditions specific to small arteries and arterioles. The initial coordinate

$$y_a^{max} = \frac{y^{max}}{a} \tag{6}$$

was normalized to the radius of wire. The maximum capturing distance (MCD) was defined as the maximum value of the initial coordinate (i.e., the furthest point away from the wire) where the MMP (cluster) could still be captured on the blood vessel's wall. The MCD was calculated for the differing system parameters described in the previous section, thus enabling optimal process conditions for capturing and hence depositing of MMPs in a blood vessel.

Using the Newton−Raphson method (*28*) eqs 4 and 5 were numerically solved, enabling the shape and size of the stable deposits to be determined. The maximum size of the deposits was calculated by varying the differing values of the process parameters described above to enable the opportunity of maximum embolization.

Results and Discussion

(a) Model Simulations of the Motion and Deposition of MMPs. Figure 3 presents specific trajectories at the limit of capture (MCD) into an artery, for the motion of the MMPs and their clusters in the region of nonuniform magnetic field, close to the magnetized ferromagnetic wire. Figure 3a shows the trajectories for MMPs with low magnetic susceptibility ($\chi = 0.25$) and Figure 3b for high magnetic susceptibility ($\chi = 1.6$). It can be readily seen that the influence of the magnetic force is larger when it acts on clusters than on a single particle.

To ensure the capture of all particles, it was necessary to increase the magnetic susceptibility of particles so that the MCD (y_a^{max1}), corresponding to a single particle

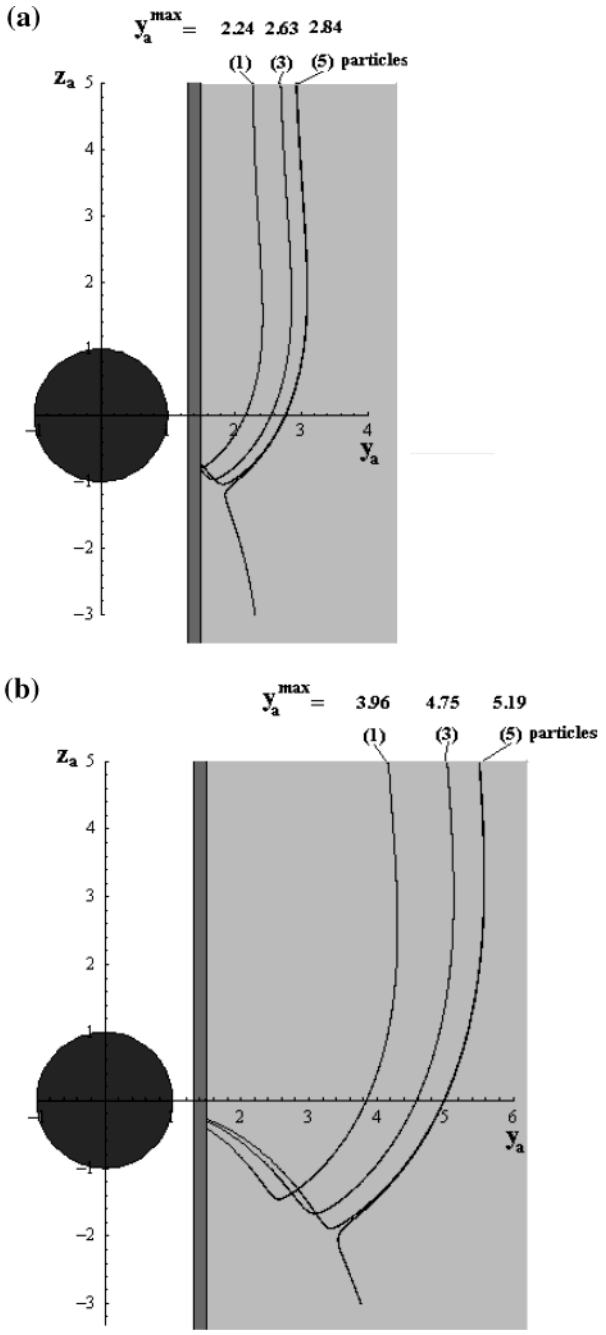

Figure 3. Specific trajectories at the limit of capture (MCD) for a single particle (1) and for clusters of three (3) and five (5) particles, respectively, for (a) low magnetic susceptibility ($\chi = 0.25$) and (b) high magnetic susceptibility ($\chi = 1.6$) MMPs. Model parameters: $a = 5 \times 10^{-4}$ m, $b = 2.25 \times 10^{-6}$ m, $K = 0.9$, $H_0 = 64 \times 10^4$ A/m, $\eta_f = 0.028$ kg/ms, $v_0 = 5 \times 10^{-2}$ m/s.

capture, be greater than the diameter of the artery ($D_a = D/a$), namely, $y_a^{max1} > D_a + 1.3$. The constant 1.3 is the normalized distance between the wire's axes and the artery's wall adjacent to wire. This distance can have a larger value, but accordingly, the efficiency of magnetic action on MMPs carried by blood decreases at larger distances. For the conditions specified in Figure 3 the absolute values of MCD for a single particle $= D_a \cdot a =$ 2.24·0.5 mm = 1.12 mm ($\chi = 0.25$) and similarly 1.98 mm ($\chi = 1.6$). This means that all particles having larger magnetic susceptibilities will be captured on the vessel's wall when its diameter is $D \approx 1-1.5$ mm or less. These estimated values of MCD may be slightly different from the real ones, depending on the concentration of MMPs and the relationship between blood flow velocity, vessel dimensions, and blood pressure.

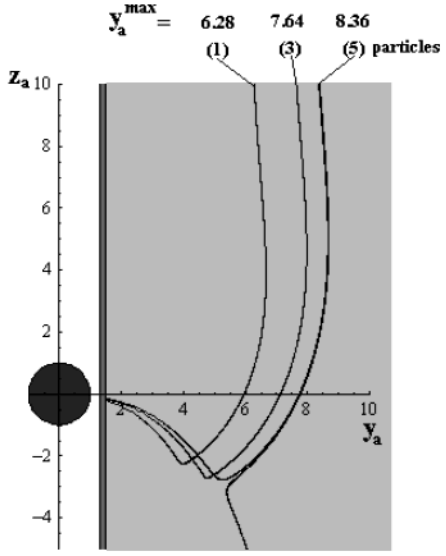

Figure 4. The trajectories of particles in a small artery, for a flow velocity of $v_0 = 2.5 \times 10^{-2}$ m/s. Model parameters: $a = 2.5 \times 10^{-4}$ m, $b = 0.5 \times 10^{-6}$ m, $\chi = 80$, $K = 0.9$, $H_0 = 40 \times 10^4$A/m, $\eta_f = 0.028$ kg/ms.

Figure 4 presents the trajectories at the capturing limit (MCD) of MMPs and their clusters for a smaller artery, where the velocity of blood ($v_0 = 2.5 \times 10^{-2}$ m/s) is a factor of 2 smaller than in the previous case.

Even though the intensity of the background magnetic field and the size of the particles are smaller than those used for the simulation from Figure 3b, the absolute value of MCD for singular particles ($y^{max1} = a \cdot y_a^{max1} \cong$ 1.41 mm) was comparable with that obtained for the above case ($y^{max1} \cong 1.98$ mm). This was possible because the magnetic force acting on the particles increases with the magnetic susceptibility of particles ($\chi = 80$). Also, the slower velocity of blood enhances the capture of particles. If the velocity of blood was double, then capturing conditions similar to those from Figure 3b would be obtained when the intensity of background magnetic field was increased to $H_0 \cong 90 \times 10^4$ A/m. Practically it is more convenient to use realistic values for the magnetic field ($H_0 \cong 40 \times 10^4$ A/m), associated with greater MMP radius ($b = 10^{-6}$ m) and higher magnetic susceptibility ($\chi = 80$). Also, increasing the concentration of the particles will induce their clustering and hence increase the MCD.

(b) Model Simulations of the Stability and Limit of MMPs Deposits. Figure 5 presents transversal sections drawn through stable deposits of particles that build up on the wall of a blood vessel, adjacent to the ferromagnetic wire at the limit of saturation of particle buildup.

It can be seen that for both types of particles ((a) $\chi =$ 0.25, (b) $\chi = 1.6$) the deposits have unsymmetrical shapes. This is due to different relative orientations of the tangential magnetic force and the hydrodynamic drag force in the 1st and 4th quadrants. The forces have the same direction in the 1st quadrant and consequently the MMPs roll toward the Oy_a axes, whereas the forces have opposite directions in the 4th quadrant where the tangential component of magnetic force is oriented toward the Oy_a axes, which inhibits the rolling of MMPs downstream of the wire, resulting in greater numbers of MMPs being retained below the Oy_a axes.

It is also readily seen that the buildup increases when the magnetic susceptibility of MMPs increases. This

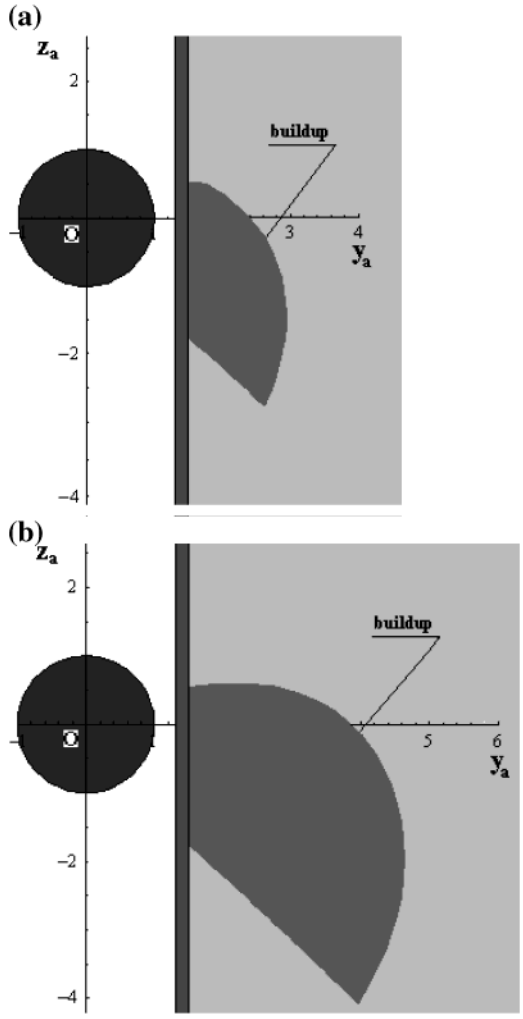

Figure 5. Simulation of MMP deposits in a blood vessel for MMPs with different magnetic properties: (a) $\chi = 0.25$, (b) $\chi = 1.6$. Process parameters as in Figure 3.

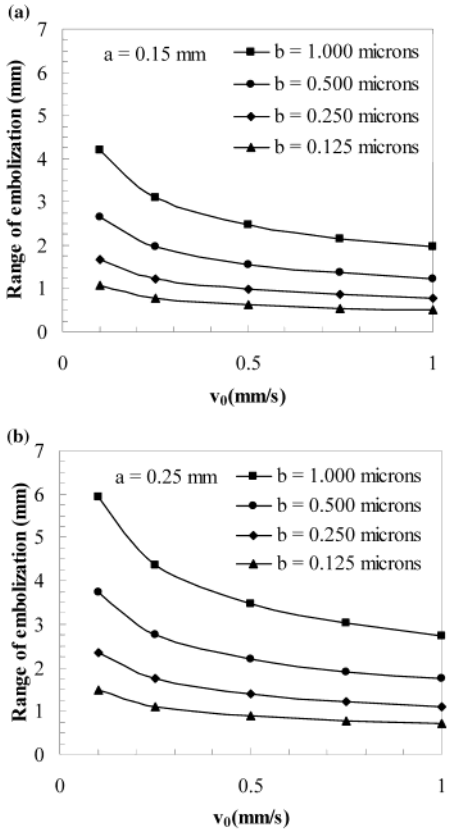

Figure 6. The range of embolization for magnetite particles of different sizes, various values of blood velocity in a human tumor, and different wire radii: (a) $a = 1.5 \times 10^{-4}$ m, (b) $a = 2.5 \times 10^{-4}$ m. Model parameters: $b = 0.125$ to 1.0×10^{-6} m, $M_p = 416\,000$ A/m, $K = 0.9$, $H_0 = 80 \times 10^4$ A/m, $\eta_f = 0.028$ kg/ms.

indicates that the embolizing of blood vessels can be done more efficiently when using MMPs that have large magnetic susceptibilities. However, it is plausible that the structure of the buildup may be less compact for strong MMPs, and consequently only partial sealing may occur (*17*).

Particles (1.0 and 4.5 μm diameter) used in the simulations above were considered because they are potentially suitable for embolizing of small arteries. The biodistribution of these particles entering the tumor microvasculature will be suboptimal because of possible particle clustering before entry to the tumor. To avoid this drawback, smaller particles, of nanometer size, are considered in the model. Another factor, which must be considered, is that tumors are ischemic or have erratic blood flow (*29*, *30*), which is heterogeneous both spatially and temporally and will influence particle deposition.

Consequently, Figure 6 presents the range of embolization (measured from the center of wire along the magnetic field direction) for different velocities of the blood, specific to tumor microcirculation (*30*), for magnetite particles of different sizes and using ferromagnetic wires of different radii. Using a thicker wire ($a = 0.25$ mm) the range of embolization extends from less than 1.0 mm for smaller particles ($b = 0.125$ μm) to 4.0−5.9 mm for larger ones ($b = 1.0$ μm) (Figure 6b). These results are for blood flow velocities of $v_0 = 0.1-0.5$ mm/s, which may typically be found within a tumor. The results for the range of embolization obtained for thinner wires ($a = 0.15$ mm) are approximately 30% less than in the previous case. However, it is worth noting that the MCD expressed in units of wire radii is greater for thinner wires than for thicker ones (results not shown). This was expected since the magnetic velocity of the particles (eq 3) increases with decreasing wire radius, and wires with smaller diameter will be capable to capture even superparamagnetic nanoparticles, subject to thermal fluctuations and dynamic instabilities of particle deposition. These instabilities could result in particle spreading to normal tissue. For example, thermal fluctuations becomes significant for magnetite particles less than ~0.04 μm, if the intensity of the magnetic field H_0 is less than 80×10^4A/m and the distance between particles and wire is greater than 100 μm ($a = 50$ μm, $K \approx 0.9$) (*31*).

The results presented above are consistent with ferromagnetic wires placed adjacent to the tumor site. However, if the wire is inserted into the tumor's tissue the range of embolization is increased 2-fold because the magnetic field gradient is active on both sides of the wire. Increasing the magnetic field intensity to $H_0 > 12 \times 10^6$ A/m can extend the range of embolization, or alternately the size of particles can be reduced to approximately 0.1 μm. However, from a practical point of view, high magnetic field intensities can only be obtained in narrow spaces, suitable for tests on small animals (*32*) or for tumors localized at the surface of the human body.

From the above it can be observed that the size of embolizing domain can be extended from a few mm^3 for smaller particles to a few cm^3 for larger ones, but in this later case particle concentration must be low to avoid the

clustering process before entry to the tumor (*17*, *18*). The small particles (2b = 0.1−0.25 μm) could also contain β or γ radioisotopes, and even though the embolizable volume covered by the particles is relatively small, the rays can give an improved microdosimetry for cytotoxic therapy following the embolic therapy. For example, the β radiation emitted by ^{188}Re radioisotopes, bound to MMPs, can destroy tumor cells up to a range of 11 mm in tissue, as reported in ref 20. Encouraging results has been also obtained in treatment of squamous cell carcinoma in rabbits, using ferrofluids (0.1 nm magnetite particles bound to mitoxantrone (FF-MTX)) that were concentrated in a high intensity and low gradient magnetic field (*32*). The authors reported that the animals treated by intra-arterial injection with 20% FF-MTX had a 50% reduction in volume of tumor after 3−12 days (mean, 6 days) and complete tumor remission between the 15th and 36th day (mean, 26 days) after treatment. Histological analyses of the targeted tissue show that the magnetic particles were found on the endothelium nearest the highest magnetic field, in the tumor interstitium, and in the adjacent normal tissue. We believe that increasing the gradient of the magnetic field using ferromagnetic needles will improve the particle concentration on the tumor site. It has also been reported (*33*) that magnetic targeting tests of thermosensitive magnetoliposomes to mouse livers have been made in an in situ on-line perfusion system. A 73−80% holding of magnetic particles has been obtained using bar permanent magnets. The results above demonstrate the potential of ferromagnetic wires to improve the recovery of particles approaching 100%. Moreover, the method could be more useful in targeting of magnetic particles to tumors from large animals, where the control of the blood flow and particle motion to the target region is difficult to realize (*34*).

Conclusions

By modeling magnetized ferromagnetic wires to obtain magnetic fields with high gradient it has been possible to simulate the deposit and stability of MMPs carried by blood onto the walls of a blood vessel. This technique may be useful in tumor therapies, for target areas that are improper for surgery or are difficult to access by procedures using catheters or radiopharmaceutical agents.

For the operational parameters used in this work, the analysis of MMPs trajectories shows that the MCD takes values of between 2 and 8 times the radius of the ferromagnetic wire (0.5−2.0 mm) for large superparamagnetic particles and relative large flow rates (2.5−5.0 cm/s). It has been proven that the MCD is larger for clusters of MMPs than for single particles. The MCD also increases with the magnetic susceptibility of the MMPs, the number of particles in a cluster, and the intensity of the magnetic field.

It was found that the deposits of particles at the limit of saturation have unsymmetrical shape. Also, the size of the deposit depends on the values of the process parameters and in particular the magnetic susceptibility of the MMPs. Similarly as for particle motion modeling, it is expected that the size of the deposit increases with increasing intensity of magnetic field, size of particles, and radius of wire.

An extrapolation of the model when the forces and their moments are in equilibrium acting on magnetite inserted into a system of arterioles showed the range of embolization to be 4−28 times greater than the radius of the ferromagnetic wire (embolization range 1.0−6.0 mm) depending on modeling parameters of blood flow, particle size, wire radius, and intensity of magnetic field. However, we are cautious about the applicability of this variant of the model for embolizing of systems of arterioles, and experimental validation is necessary. In addition further theoretical modeling and experimental work is necessary to compare the effect of cluster formation with and without the acupuncture needle to see how this affects the range of embolization.

Acknowledgment

This work was funded by Romanian Ministry of Education and Research (contract 43/2002) and by EU Marie Curie Fellowship (contract QLK6-CT-2002-51544). The authors gratefully acknowledge helpful discussions with Prof. Urs Hafeli from The Cleveland Clinic Foundation, Cleveland, OH, from which we started this study, and Dr. Vasile Badescu from National Institute of R&D of Technical Physics, Iasi, Romania for helpful discussions on the magnetic capture process.

References and Notes

(1) Pieters, B. R.; Williams, R. A.; Webb, C. *Colloid and Surface Engineering: Applications in the Process Industries*; Williams, R. A., Ed.; Butterworth-Heinemann Ltd.: Oxford, 1992; p248.

(2) Safarik, I.; Safarikova, M.; Forsythe, S. J. The application of magnetic separations in applied microbiology. *J. Appl. Bacteriol.* **1995**, *78*, 575−585.

(3) Safarik, I.; Safarikova, M. Use of magnetic techniques for the isolation of cells. *J. Chromatogr. B* **1999**, *722*, 33−53.

(4) Thiel, A.; Scheffold, A.; Rodbruch, A. Immunomagnetic cell sorting−pushing the limits. *Immunotechnology* **1998**, *4* (*2*), 89−105.

(5) Ugelstad, J.; Prestvik, W. S.; Stenstad, P.; Kilaas, L.; Kvalheim, G. *Magnetism in Medicine: A Handbook*; Andra, W., Novak, H., Eds.; Wiley-VCH: Berlin, 1998; p 471.

(6) Strachan, N. J. C.; MacRae, M.; Hepburn, N. F.; Rotariu, O.; Ogden, I. D. Can a Rapid Method Detect the Presence of *E. coli* O157 in Food, Veterinary and Agricultural Samples within a Working Day? *Proceedings of the 4th International Symposium on Shiga Toxin (Verocytotoxin) producing E. coli Infections*, Oct 29−Nov 2, Kyoto, Japan, 2000; p 87.

(7) Moore, L. R.; Zborowski. M.; Sun, L.; Chalmers, J. J. Lymphocyte fractionation using immunomagnetic colloid and a dipole magnet flow cell sorter. *J. Biochem. Biophys. Methods* **1998**, *37*, 11−33.

(8) Haik, Y.; Pai, V.; Chen, C.-J. Development of magnetic device for cell separation. *J. Magn. Magn. Mater.* **1999**, *194* (1−3), 254−261.

(9) Ruuge, E. K.; Rusetski, A. N. Magnetic fluids as drug carriers: Targeted transport of drugs by a magnetic field. *J. Magn. Magn. Mater.* **1993**, *122* (1−3), 335−339.

(10) Babincova, M.; Altanerova, V.; Lambert, M.; Altaner, C.; Sramka, M.; Machova, E.; Babinec, P. Site specific in vivo targeting of magnetolipozomes in external magnetic field. Z. *Naturforsch.* **2000**, *55c*, 278−282.

(11) Lube, A. S.; Bergeman, C.; Riess, H.; Schriever, F.; Reichardt, P.; Possinger, K.; Matthias, M.; Dorken, B.; Herrmann, F.; Gurtler, R.; Hohenberger, P.; Haas, N.; Sohr, R.; Sander, B.; Lemke, A. J.; Ohlendorf, D.; Huhnt, W.; Huhn, D. Clinical experiences with magnetic drug targeting: a phase I study with 4′-epidoxorubicin in 14 patients with advanced solid tumors. *Cancer Res.* **1996**, *56*, 4686−4693.

(12) Goodwin, S.; Peterson, C.; Hoh, C.; Bittner, C. Targeting and retention of magnetic targeted carriers (MTCs) enhancing intra-arterial chemotherapy. *J. Magn. Magn. Mater.* **1999**, *194* (1−3), 132−139.

(13) Liberti, P. A.; Rao, C. G.; Terstappen, L. W. M. M. Optimization of ferrofluids and protocols for the enrichment of breast tumor cells in blood. *J. Magn. Magn. Mater.* **2001**, *225* (1−2), 301−307.

(14) Hafeli, U. O.; Pauer, G. J.; Roberts, W. K.; Humm, J. L.; Macklis, R. M. *Scientific and Clinical Applications of Mag-*

netic Carriers; Häfeli, U., Schütt, W., Teller, J., Zborowski, M., Eds.; Plenum Press: New York, 1997; p 501.
(15) Babincova, M.; Cicmanek, P.; Altanerova, V.; Altaner, C.; Babinec, P. AC-magnetic field controlled drug release from magnetoliposomes: Design of a method for site specific chemotherapy. *Bioelectrochemistry* **2002**, *55*, 17−19.
(16) Spies, J.; Warren, E.; Mathias, S.; Walsh, S.; Roth, A.; Pentecost, M. Uterine fibroid embolization: measurement of health-related quality of life before and after therapy. *J. Vasc. Interv. Radiol.* **1999**, *10*, 1293−1303.
(17) Sheng, R.; Flores, G. A.; Liu, J. In vitro investigation of a novel cancer therapeutic method using embolizing properties of magnetorheological fluids. *J. Magn. Magn. Mater.* **1999**, *194* (1−3), 167−175.
(18) Liu, J.; Flores, G. A.; Sheng, R. In vitro investigation of blood embolization in cancer treatment using magnetorheological fluids. *J. Magn. Magn. Mater.* **2001**, *225* (1−2), 209−217.
(19) Oberteuffer, J. A. Magnetic separation: A review of principles, devices, and aplications. *IEEE Trans. Magn.* **1974**, *10*, 223−238.
(20) Häfeli, U.; Pauer, G.; Failing, S.; Gilles, T. Radiolabeling of magnetic particles with rhenium-188 for cancer therapy. *J. Magn. Magn. Mater.* **2001**, *225* (1−2), 73−78.
(21) Babincova, M.; Babinec, P.; Bergemann, C. High gradient magnetic capture of ferrofluids: Implications for drug targeting and tumor embolization, Z. *Naturforsch.* **2001**, *56c*, 909−901.
(22) Rotariu, O.; Strachan, N. J. C. Magnetic field induced order in assemblies of superparamagnetic carrier particles. *Powder Technol.* **2003**, *132*, 226−232.
(23) Watson, J. H. P. Theory of capture of particles in magnetic high-intensity filters. *IEEE Trans. Magn.* **1975**, *11* (5), 1597−1599.
(24) Bădescu, V.; Rotariu, O.; Murariu, V.; Rezlescu, N. Magnetic capture modelling for a transversal high gradient filter cell with bounded flow field. *Int. J. Appl. Electrom.* **1996**, *7*, 57−67.
(25) Nesset, J. E.; Finch, J. A. A static model of high gradient magnetic separation based on forces within the fluid boundary layer. *Proc. Int. Conf. Ind Appl. Magn. Sep.*, Rindge, NH, 1978, Publication IEEE **1979**, *78CH1447-2MAG*, 188−195.
(26) Maass, W.; Duschl, M.; Hoffmann, H.; Friedlaender, F. J. A new model for the explanation of the saturation buidup in the transverse HGMS-configuration. *Appl. Phys. A* **1983**, *32*, 79−85.
(27) Press, W. H.; Teukolsky, S. A.; Vetterling, W. T.; Flannery, B. P. *Numerical Recipes in Fortran. The Art of Scientific Computing*, 2nd ed.; Cambridge University Press: New York, 1992; p 704.
(28) Press, W. H.; Teukolsky, S. A.; Vetterling, W. T.; Flannery, B. P. *Numerical Recipes in Fortran. The Art of Scientific Computing*, 2nd ed.; Cambridge University Press: New York, 1992; p 355.
(29) Jain, R. K. Determinants of tumor blood flow: a review. *Cancer Res.* **1988**, *48*, 2641−2658.
(30) Jain, R. K. Delivery of molecular and cellular medicine to solid tumors. *Adv. Drug Delivery Rev.* **2001**, *46*, 149−168.
(31) Gerber, R.; Takayasu, M.; Friedlaender, F. J. Generalization of HGMS theory: the capture of ultra-fine particles. *IEEE Trans. Magn.* **1983**, *19*, 2115−2117.
(32) Alexiou, C.; Arnold, W.; Klein, R. J.; Parak, F. G.; Hulin, P.; Bergemann, C.; Erhardt, W.; Wagenpfeil, S.; Lübbe, A. S. Locoregional cancer treatment with magnetic drug targeting. *Cancer Res.* **2000**, *60*, 6641−6648.
(33) Viroonchatapan, E.; Sato, H.; Ueno, M.; Adachi, I.; Tazawa, K.; Horikoshi, I. Magnetic targeting of thermosensitive magnetoliposomes to mouse livers in an in situ on-line perfusion system. *Life Sci.* **1996**, *58* (24), 2251−2261.
(34) Moroz, P.; Jones, S. K.; Gray, B. N. Arterial embolization hyperthermia in porcine renal tissue. *J. Surg. Res.* **2002**, *105*, 209−214.

Accepted for publication August 14, 2003.

BP034146O